Available online at www.sciencedirect.com

ScienceDirect

IFAC Papers Online CONFERENCE PAPER ARCHIVE

IFAC-PapersOnLine 49-3 (2016) 297–302

Dynamic Model for estimating the Macroscopic Fundamental Diagram ⋆

Hoai-Nam Nguyen * **Barak Fishbain** ** **Eilyan Bitar** ***
David Mahalel **** **Per-Olof Gutman** †

* *IFP Energies nouvelles, Rond-point de l'echangeur de Solaize, BP 3, 69360 Solaize - France. (e-mail: hoai-nam.nguyen@ifp.fr)*
** *Faculty of Civil and Environmental Engineering, Technion - Israel Institute of Technology, Haifa 32000, Israel. (e-mail: fishbain@technion.ac.il)*
*** *Department of Electrical and Computer Engineering Cornell University, Ithaca, NY, USA. (email: eyb5@cornell.edu)*
**** *Faculty of Civil and Environmental Engineering, Technion - Israel Institute of Technology, Haifa 32000, Israel. (e-mail: mahalel@technion.ac.il)*
† *Faculty of Civil and Environmental Engineering, Technion - Israel Institute of Technology, Haifa 32000, Israel. (e-mail: peo@technion.ac.il)*

Abstract: The Macroscopic Fundamental Diagram (MFD) relates the number of circulating vehicles (or accumulation) to a neighbourhood's average speed or flow. In theory the MFD has a well-defined maximum which remains invariant over time. Recent studies, however, suggest that in practice this is not the case, and the MFD does present a variations over time. These variations in the MFD render traffic simulations, modelling and control schemes inaccurate, as these tools do not capture the dynamic nature of the MFD. This paper presents a dynamic model for estimating the MFD, so it does capture the MFD's time varying nature. A mathematical Kalman-filter based framework for solving the model and estimating the MFD are also presented. The application of the method on a small scale example shows the potential of the method.

Keywords: Macroscopic Fundamental Diagram (MFD); Traffic Network State; Dynamic Estimation; Traffic Control; Kalman-Filter

1. INTRODUCTION

Transportation infrastructure systems are critical to serving the needs of millions of people. Traffic congestion represents one of the major obstacles to an efficient operation. In 2011, congestion caused urban Americans to travel 5.5 billion hours more and to purchase an extra 2.9 billion gallons of fuel for a congestion cost of $121 billion, 0.7% of the US GDP Schrank et al. (2012). This problem will only worsen as the growth in demand has far outstripped the rate of installed highway capacity. In fact, the US Federal Highway Administration estimates that the number of vehicle miles traveled increased by 76% from 1980 to 1999, while total miles of installed highway capacity increased by only 1.5% Noland and Cowart (2000). These challenges are further exacerbated by population growth, concentrated demand due to urbanization, and depletion of natural resources Rosenberg et al. (2010). Thus, arises the need for better understanding and utilization of the transportation network.

Since the seminal work of Greenshields et al. (1933), the fundamental diagram has become one of the most common tools for modelling a road segment and it flow-density, speed-flow, and speed-density relations (e.g., Dervisoglu et al. (2009); Helbing (2009); Wu et al. (2011)). The fundamental diagram was the base for many studies, starting from the work of Lighthill and Whitham (1955) and Richards (1956), through the work of Gerlough and Huber (1975) all the way to the work on the cell-transmission model (CTM) Daganzo (1994, 1995), which adopted a simplified fundamental diagram. All the aforementioned work sought the fundamental diagram to time invariant.

Recent advances in computational, sensory and communication technologies have enabled the analysis of a network segment, rather than a single stretch. To this end, the following studies: Daganzo and Geroliminis (2008); Geroliminis and Daganzo (2007, 2008) showed, through the moving observer method, that the fundamental diagram can serve as a tight bound for the average flow-density states of any urban street or network. This work essentially has extended the use of the fundamental diagram from a single

⋆ This research was supported in part by the Ruch collaboration grant through the Jacobs Technion-Cornell Institute. The first author thanks the U.S.-Israel Binational Science Foundation and the Technion Zeff fellowship. The second author acknowledges the fundings of the Glasberg-Klein, the NY Metropolitan Research Foundations, the Israeli Environmental and Health Foundation and The Technion Center of Excellence in Exposure Science for their partial financial support to this research.

10.1016/j.ifacol.2016.07.050

road segment to a network. They dubbed this extension as the Macroscopic Fundamental Diagram (MFD). Using the MFD concept, traffic control is simplified enormously as it offers an aggregate model approach that considers the traffic dynamics of a large urban area. Their analysis, however, assumed time invariant road conditions and homogenous spatial distribution of vehicle density over the network Geroliminis and Sun (2011).

While the fundamental diagram is sought to be time invariant, many studies have shown that this is not the case for the MFD. Ji et al. (2010) showed, by utilising a microscopic simulation model, that the MFD shape is a property not only of the network itself but also of the applied traffic control measures, congestion and traffic demand. Thus, traffic itself has an effect on the concurrent MFD shape. Mazloumian et al. (2010) examined vehicle density and its variability and its effect on urban traffic network performance. They found the variability to be a key factor in the process. Saberi and Mahmassani (2012) investigated the impact of the spatial and temporal distribution of congestion in a network on the shape and properties of the flow-density relation. The research showed that the maximum network average flow is not a constant value but varies across different days. In addition, for the same value of average network occupancy, a variation of occupancy was observed. The variation was attributed to the formation of fragmented queues and traffic instability. Variability was also observed when the spatial distribution of densities over the network was inhomogeneous and the average network occupancy remained consistently high and roughly unchanged for successive time intervals. Knoop et al. (2012) recapitulated this notion and acknowledged that the MFD does change over time. In a later work Knoop et al. (2013) the impact of traffic dynamics on the MFD was explored. The latter showed that the network flow is not constant for a fixed number of vehicles as predicted by the MFD, but decreases due to local queuing and spill back processes around the congestion. Following the above body of work, we conclude that the MFD is time variant and is affected by time variant factors such as the concurrent traffic conditions.

One of the first applications of the MFD were its utilization in traffic network dynamic control. Zheng et al. (2012) presented a dynamic pricing scheme, where tolls are controlled by an MFD. Geroliminis et al. (2013) used an MFD-based control mechanism to govern traffic flow between two urban regions such that the number of trips that reach their destinations is maximized. Zhang et al. (2013) presented the use of the MFD for achieving optimal adaptive traffic signal system. While all these applications present an unprecedented tool for managing and controlling transportation facilities, they all assumed time invariant MFD. Thus, the dynamic nature of the MFD, as traffic state changes, has not been regarded. Using inaccurate (or outdated) MFD to describe the network in question, results in a suboptimal control and underutilization of the network. Therefore, there is a great need to generate a mechanism that follows traffic conditions and distribution over the network and updates the MFD accordingly.

In this paper, a new mechanism to update the MFD in an on-line fashion, through polynomial Kalman filter Zarchan and Musoff (2005), is presented. Such a filter allows to avoid the large computational cost usually required by other approaches such as extended Kalman or particle filters. Further, the polynomial Kalman Filter allows for capturing the time varying nature of the MFD. Previous studies that aimed at estimating the MFD Daganzo and Geroliminis (2008); Geroliminis and Daganzo (2008, 2007); Xie et al. (2013); Gayah and Dixit (2013); Knoop and Hoogendoorn (2013) did not account for temporal variability, which manifested itself in a scattered pattern. For example, Gayah and Dixit (2013) introduced a methodology to estimate the MFD from in traffic agents monitoring. Their work was shown accurate when the network is congested, and less so, when the network was uncongested. Ojeda et al. (2013) suggested Kalman filtering for estimating road density. Their work estimated the density state given MFD fixed model and stochastic perturbations. Therefore we conclude that the MFD does change with traffic and when the network is uncongested, there is a small number of agents to get accurate estimation of traffic.

Thus, the contribution of this paper is twofold: (i) it presents a model for a continuous updating of the MFD in traffic control applications, as traffic changes; and (ii) it introduces a simple, yet efficient, mechanism for updating the MFD as measurements acquired from the network are gathered. Finally, a demonstration of the suggested scheme is given on a real-life network. The paper is organized as follows. The MFD concept is presented in Section 2. In Section 3, the design of the MFD based on the polynomial Kalman filter is addressed, whereby a various estimation schemes are proposed and discussed. Then Section 4 describes the data processing. Several key issues concerning MFD estimation are carefully investigated in Section 5. Finally, Section 6 draws some conclusions and future work.

2. MACROSCOPIC FUNDAMENTAL DIAGRAM

The macroscopic fundamental diagrams have been proven to exist in small networks, relating the local flow and density Geroliminis and Daganzo (2007). A typical schematic MFD is illustrated in Figure 1. The MFD describes the

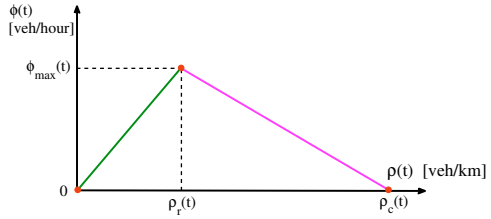

Fig. 1. Macroscopic fundamental diagram.

transition of the road network between three states: *Free flow* - When the density is low and the the flow $\phi(t)$ is undisturbed. This stage is described by the green part shown in Figure 1. With the increase of the number of vehicles, $\phi(t)$ rises up to the maximum, indicated by the point $(\rho_r(t), \phi_{max}(t))$, called the *sweet spot* or *critical density*. As the number of vehicles further increases, passengers will

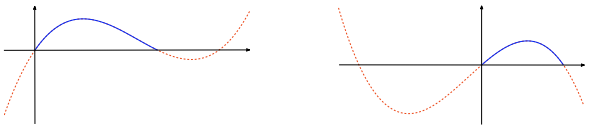

(a) $\alpha_3 > 0$ (b) $\alpha_3 < 0$

Fig. 2. 3^{rd} order polynomial MFD approximation - $\phi(t)$ as a function of $\rho(t)$

experience delay. If vehicles continue to enter the network, it will result in a congestion state where vehicles block each other and the flow declines, indicated by the magenta part in Figure 1.

3. RECURSIVE ESTIMATION OF MACROSCOPIC FUNDAMENTAL DIAGRAM

3.1 The model

There are many functional forms to describe the shape of the MFD in the flow density plane. A polynomial form is chosen for reasons of simplicity. In this form, the coefficients of determination can be found by using linear least square or Kalman filter approaches.

In general, the function $\phi(\rho)$ should have an order of more than two. To see this, one can consider a polynomial function of the order two. Due to the symmetric property of this function, the density $\rho_r(t)$ of the *sweet spot* point can be computed as

$$\rho_r(t) = \frac{\rho_c(t)}{2} \tag{1}$$

where $\rho_c(t)$ is the density of the standstill point, see Figure 1. Since this is typically not the case, the function $\phi(\rho)$ should have an order of more than two. A third order polynomial function is chosen as it is the simplest non-symmetric, linear-in-the-parameters model for which the Kalman filter is easy to work with. It is also known that the density $\rho(t) = 0$ should give the zero flow. In the result, the following equation is obtained,

$$\phi(t) = \alpha_1\rho(t) + \alpha_2\rho^2(t) + \alpha_3\rho^3(t) \tag{2}$$

It is useful to calculate the derivative of the flow $\phi(t)$ with respect to the density $\rho(t)$,

$$\frac{d\phi}{d\rho} = \alpha_1 + 2\alpha_2\rho(t) + 3\alpha_3\rho^2(t) \tag{3}$$

Clearly, $\alpha_1 > 0$, since $\frac{d\phi}{d\rho}$ is positive at $\lim \rho(t) \to 0^+$.

There are two cases which correspond to $\alpha_3 > 0$ and $\alpha_3 < 0$, where the function (2) can have the MFD shape. They are illustrated in Figure 2a and Figure 2b.

For the case $\alpha_3 > 0$, using Figure 2a, it follows that

- The function (2) has a local maximum and a local minimum at densities greater than zero, while the density at the local maximum is less than the density at the local minimum.
- The function (2) has three roots, one root is zero and two other roots are greater than zero. The density at the standstill point corresponds to the positive smallest root.
- Using the Vieta's theorem Vinberg (2003), it follows that $\alpha_2 < 0$ since the function (2) has three non-negative roots and the the assumption this case that $\alpha_3 > 0$.

Analogously, for the case $\alpha_3 < 0$, from Figure 2b, it is clear that

- The function (2) has the local maximum at the density greater than zero and the local minimum at the density smaller than zero.
- The function (2) has three roots, one root is less than zero, one root is zeros and one root is greater than zero. The density at the standstill point corresponds to the positive root.

The density of the sweet spot point $\rho_r(t)$ and the density at the standstill point $\rho_c(t)$ can be computed as follows,

- If $\alpha_3 > 0$, $\rho_r(t)$ is the positive smallest root of the following equation

  $$\alpha_1 + 2\alpha_2\rho(t) + 3\alpha_3\rho^2(t) = 0$$

  Hence

  $$\rho_r(t) = \frac{-\alpha_2 - \sqrt{\alpha_2^2 - 3\alpha_1\alpha_3}}{3\alpha_3} \tag{4a}$$

  And $\rho_c(t)$ is the positive smallest root of the following equation

  $$\alpha_1 + \alpha_2\rho(t) + \alpha_3\rho^2(t) = 0$$

  Hence

  $$\rho_c(t) = \frac{-\alpha_2 - \sqrt{\alpha_2^2 - 4\alpha_1\alpha_3}}{2\alpha_3} \tag{4b}$$

- If $\alpha_3 < 0$, analogous to equation (4), (4b), the densities at the sweet spot point and at the standstill point are computed as follows

  $$\rho_r(t) = \frac{-\alpha_2 - \sqrt{\alpha_2^2 - 3\alpha_1\alpha_3}}{3\alpha_3} \tag{5a}$$

  $$\rho_c(t) = \frac{-\alpha_2 - \sqrt{\alpha_2^2 - 4\alpha_1\alpha_3}}{2\alpha_3} \tag{5b}$$

Using equations (4) and (5), it is worth noticing that $\rho_r(t)$ and $\rho_c(t)$ have the same expression, regardless of the sign of α_3. Thus, the consideration of the sign of α_3 does affect the computational flow and complexity.

The interpretation of α_1, α_2, α_3 as well as $\rho_r(t)$, $\rho_c(t)$ and $\phi(t)$ for traffic characteristics is shown in Table 1:

Table 1. Interpretation of the variables

Description	Symbol	Equation	Unit
1st order term	α_1		$km/hour$
2nd order term	α_2		$km^2/(veh \times hour)$
3rd order term	α_3		$km^3/(veh^2 \times hour)$
Sweet spot density	$\rho_r(t)$	Eq. (5a)	veh/km
Sweet spot flow	$\phi_{max}(t)$	$\phi(\rho_r(t))$	$veh/hour$
Standstill density	$\rho_c(t)$	Eq. (5b)	veh/km

Defining

$$\begin{cases} \boldsymbol{\alpha} &= [\,\alpha_1\ \alpha_2\ \alpha_3\,]^T, \\ \boldsymbol{c}(t) &= [\,\rho(t)\ \rho^2(t)\ \rho^3(t)\,]^T, \\ y(t) &= \phi(t) \end{cases}$$

Equation (2) can be rewritten as

$$y(t) = \boldsymbol{c}(t)^T\boldsymbol{\alpha} \tag{6}$$

3.2 Recursive least squares and the Kalman filter approach

In least square estimation unknown parameters are chosen in such a way that the sum of the squares of the difference between the actually observed and the computed values, is minimized Ljung (1999); Åström and Wittenmark (2008). This translates into finding the parameters that minimizes the following *loss-function*, for the model (3):

$$V(\boldsymbol{\alpha}, n) = \frac{1}{2}\sum_{t=1}^{n}(y(t) - \boldsymbol{c}(t)^T\boldsymbol{\alpha})^2 \tag{7}$$

where n is the number of data points, and $y(t)$ and $c(t)$ stand for te variables measured at time t. The closed form solution to the problem (7) at time n can be obtained as follows:

$$\alpha(n) = \left(\sum_{t=1}^{n}\boldsymbol{c}(t)\boldsymbol{c}^T(t)\right)^{-1}\left(\sum_{t=1}^{n}\boldsymbol{c}(t)y(t).\right) \tag{8}$$

As far as we are interested in real-time parameter estimation, it is desirable to make the computation recursively to save computational time. Computation of the least square estimate can be arranged in such a way that the results obtained at time instant $n-1$ are updated to get the estimates at time n. The recursive form is given by Ljung (1999); Åström and Wittenmark (2008),

$$\alpha(n) = \alpha(n-1) + K(n)\left(y(n) - c^T(n)\alpha(n-1)\right) \tag{9a}$$

where

$$\begin{aligned} K(n) &= P(n)c(n) = \\ &= P(n-1)c(n)\left(I + c(n)^T P(n-1)c(n)\right)^{-1} \end{aligned} \tag{9b}$$

and

$$\begin{aligned} P(n) &= P(n-1) - P(n-1)c(n) \\ &\cdot \left(I + c(n)^T P(n-1)c(n)\right)^{-1} c^T(n)P(n-1) \\ &= (I - K(n)c^T(n))P(n-1) \end{aligned} \tag{9c}$$

$P(n)$ is the covariance matrix (for more details on the above derivation, see Ljung (1999); Åström and Wittenmark (2008)).

In the least square model (6), the estimates α are assumed to be constant. However, in the MFD model, the parameters may vary depending on the traffic conditions. One pragmatic approach in this case is simply to replace the least squares criterion (7) with

$$V(\alpha, n) = \frac{1}{2}\sum_{t=1}^{n}\lambda^t(y(t) - c(t)^T\alpha)^2 \tag{10}$$

where $0 < \lambda \leq 1$ is called the forgetting factor. It operates as a weight which diminishes for the more remote measurement data. The scheme is known as least-square with exponential forgetting and $\alpha(n)$ can also be calculated recursively using the same update equation (9a) but with different $K(n)$ and $P(n)$, see for example Ljung (1999); Åström and Wittenmark (2008). A main disadvantage of exponential forgetting is that data is discounted even if $y(n)$ does not contain any new information about the parameter α Åström and Wittenmark (2008).

An alternative approach of dealing with time-varying parameters is to use the Kalman filter approach Grewal and Andrews (2011) for the following random walk model,

$$\begin{cases} \alpha(t+1) = \alpha(t) + w(t), \\ y(t) = c(t)^T\alpha(t) + v(t) \end{cases} \tag{11}$$

where $\{w(t)\}$ and $\{v(t)\}$ are discrete-time Additive White Gaussian Noise with covariances

$$E(w(t)w^T(k)) = R\delta_{tk},\ E(v(t)v^T(k)) = Q\delta_{tk}$$

where δ_{tk} is the Kronecker delta:

$$\delta_{tk} = \begin{cases} 1, & \text{if } t = k, \\ 0, & \text{if } t \neq k, \end{cases},$$

and the matrices $R \succ 0$ and $Q \succ 0$ are tuning parameters in our case. The least squares estimator will then be the Kalman filter.

The algorithm of the Kalman filter approach is summarized as follows

$$\alpha(n) = \alpha(n-1) + K(n)(y(n) - c^T(n)\alpha(n-1)) \tag{12a}$$

where

$$K(n) = S(n-1)c(n)(c^T(n)S(n-1)c(n) + R)^{-1} \tag{12b}$$

and

$$\begin{aligned} P(n) = {} & S(n-1) - S(n-1)c(n)\cdot \\ & \cdot(c^T(n)S(n-1)c(n) + R)^{-1}\cdot \\ & \cdot c^T(n)S(n-1) \end{aligned} \tag{12c}$$

and

$$S(n) = P(n-1) + Q \tag{12d}$$

Clearly, we need to choose an initial values for $\alpha(0)$ and $P(0)$. A good choice is $\alpha(0) = 0$ and $P(0) = 0$.

4. APPLICATION OF THE METHOD

To demonstrate the capability of the method to follow the MFD's behaviour, a synthetic traffic data derived from two assumed MFDs representing two week-days with AM and PM peaks were used. In this simulation the covariance matrices following Eq. (11) were tuned to $Q = 1 \cdot 10^{-8}$ and $R = 900$. Our extensive studies with simulations and real-life data strongly suggests that weather conditions and other factors affect traffic and consequentially the MFD. Therefore the two days present different traffic regimes. One can think of day 1 as a clear day and day 2 as a rainy day. The input to the system - $4,404$ synthetic density and flow records representing 48 hours' worth of data, thus, a sample every 90 seconds, are presneted in Figure 3a. The corresponding MFDs for day 1 (in blue) and day 2 (in red) are given in Figure 3b. It is evident that indeed day 1 presents different MFD than day 2. Using the Kalman filter approach, described in Section 3.1, the third order polynomial model (Eq. 2) is used to approximate the MFD.

Figure 4a presents $\alpha(t)$ as a function of time. It is evident that the α coefficients do change over time. Similar notion is observed in Figure 4b,which presents sweet spot density and flow as a function of time. Similarly to the conclusion that was drown from Figure 4a, the sweet spot parameters do change over time. It is worthwhile noting the big changes in the α coefficients and in ρ and ϕ. These changes occur in the transient between the two traffic regimes, i.e., the two days. There are several methods to overcome this and we do expect this phenomenon to be less dramatic with real data.

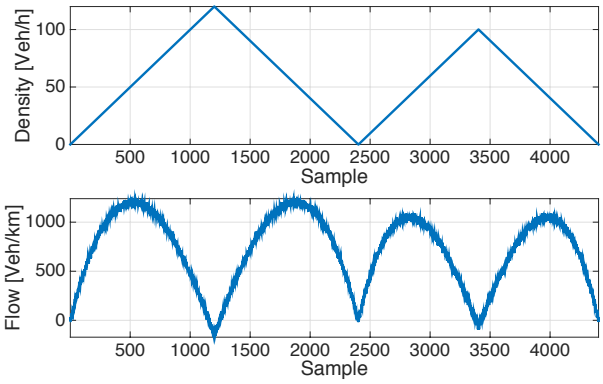

(a) Two Days Density and Flow

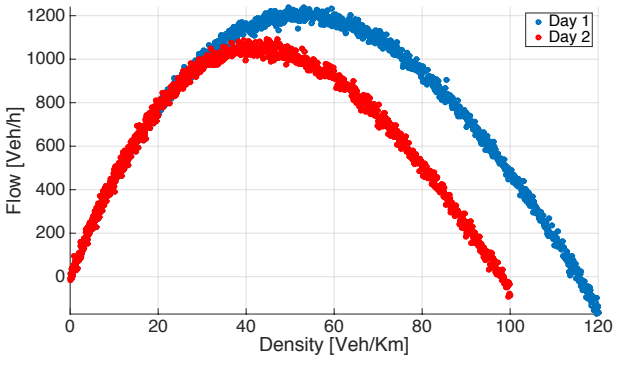

(b) MFD. Day 1 (blue) and Day 2 (red)

Fig. 3. Synthetic Traffic Data

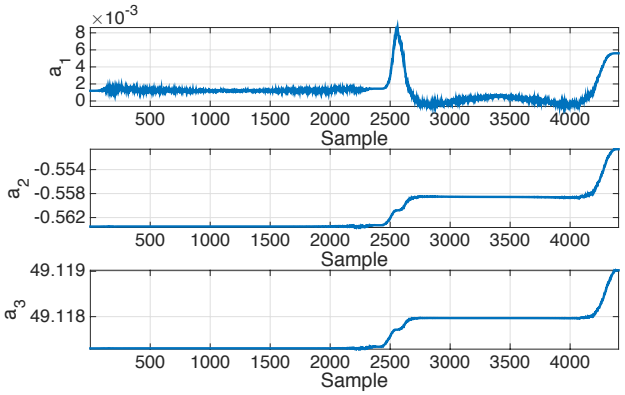

(a) $\boldsymbol{a}$ Vector Elements: a_1, a_2, a_3

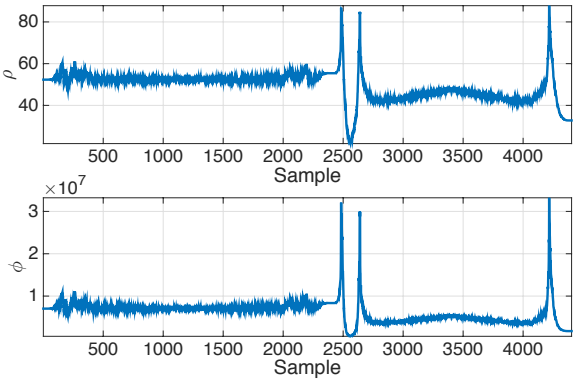

(b) Sweet spot density and flow

Fig. 4. 3^{rd} order polynomial MFD approximation

5. CONCLUSION

In this work, we show that the Microscopic Fundamental Diagram, MFD, while believed to be constant over time, it does vary. The paper provides an on-line estimation method for the MFD, using Kalman filter. Then an example of the MFD's dynamic estimations is presented. The results clearly show the time-varying nature of the MFD.

REFERENCES

Åström, K.J. and Wittenmark, B. (2008). *Adaptive control*. Dover Publications.

Daganzo, C.F. and Geroliminis, N. (2008). An analytical approximation for the macroscopic fundamental diagram of urban traffic. *Transportation Research Part B: Methodological*, 42(9), 771–781.

Daganzo, C. (1994). The cell transmission model: A dynamic representation of highway traffic consistent with the hydrodynamic theory. *Transportation Research B*, 28(4), 269–287.

Daganzo, C. (1995). The cell transmission model, part ii: Network traffic. *Transportation Research B*, 29(2), 79–93.

Dervisoglu, G., Gomes, G., Kwon, J., Horowitz, R., and Varaiya, P. (2009). Automatic calibration of the fundamental diagram and empirical observations on capacity. In *Transportation Research Board 88th Annual Meeting*, volume 15.

Gayah, V. and Dixit, V. (2013). Using mobile probe data and the macroscopic fundamental diagram to estimate network densities. *Transportation Research Record: Journal of the Transportation Research Board*, 2390, 76–86. doi:10.3141/2390-09. URL `http://dx.doi.org/10.3141/2390-09`.

Gerlough, D. and Huber, M. (1975). Traffic flow theory: A monograph. Technical report, Transportation Research Board.

Geroliminis, N., Haddad, J., and Ramezani, M. (2013). Optimal perimeter control for two urban regions with macroscopic fundamental diagrams: A model predictive approach. *Intelligent Transportation Systems, IEEE Transactions on*, 14(1), 348–359. doi: 10.1109/TITS.2012.2216877.

Geroliminis, N. and Daganzo, C.F. (2007). Macroscopic modeling of traffic in cities. In *Transportation Research Board 86th Annual Meeting*, 07-0413.

Geroliminis, N. and Daganzo, C.F. (2008). Existence of urban-scale macroscopic fundamental diagrams: Some experimental findings. *Transportation Research Part B: Methodological*, 42(9), 759–770.

Geroliminis, N. and Sun, J. (2011). Properties of a well-defined macroscopic fundamental diagram for urban traffic. *Transportation Research*

Part B: Methodological, 45(3), 605 – 617. doi: http://dx.doi.org/10.1016/j.trb.2010.11.004.

Greenshields, B., Thompson, J., Dickinson, H., and Swinton, R. (1933). The photographic method of studying traffic behavior. In *Highway Research Board Proceedings*, volume 13, 382–399.

Grewal, M.S. and Andrews, A.P. (2011). *Kalman filtering: theory and practice using MATLAB*. Wiley-IEEE press.

Helbing, D. (2009). Derivation of a fundamental diagram for urban traffic flow. *The European Physical Journal B*, 70(2), 229–241. doi:10.1140/epjb/e2009-00093-7. URL `http://dx.doi.org/10.1140/epjb/e2009-00093-7`.

Ji, Y., Daamen, W., Hoogendoorn, S., Hoogendoorn-Lanser, S., and Qian, X. (2010). Investigating the shape of the macroscopic fundamental diagram using simulation data. *Transportation Research Record: Journal of the Transportation Research Board*, 2161(1), 40–48.

Knoop, V., Hoogendoorn, S., and Lint, J.V. (2012). Routing strategies based on macroscopic fundamental diagram. *Transportation Research Record: Journal of the Transportation Research Board*, 2315, 1–10. doi:10.3141/2315-01. URL `http://dx.doi.org/10.3141/2315-01`.

Knoop, V. and Hoogendoorn, S. (2013). Empirics of a generalized macroscopic fundamental diagram for urban freeways. *Transportation Research Record: Journal of the Transportation Research Board*, 2391, 133–141. doi:10.3141/2391-13. URL `http://dx.doi.org/10.3141/2391-13`.

Knoop, V., Hoogendoorn, S., and Lint., J.V. (2013). The impact of traffic dynamics on macroscopic fundamental diagram. In *92nd Annual Meeting Transportation Research Board*.

Lighthill, M. and Whitham, J. (1955). On kinematic waves. i. flow movement in long rivers. ii. a theory of traffic flow on long crowded roads. In *Proceedings of the Royal Society, London*, volume A229, 281–345.

Ljung, L. (1999). *System identification*. Wiley Online Library.

Mazloumian, A., Geroliminis, N., and Helbing, D. (2010). The spatial variability of vehicle densities as determinant of urban network capacity. *Philosophical Transactions of the Royal Society of London A: Mathematical, Physical and Engineering Sciences*, 368(1928), 4627–4647. doi:10.1098/rsta.2010.0099.

Noland, R.B. and Cowart, W.A. (2000). Analysis of metropolitan highway capacity and the growth in vehicle miles of travel. *Transportation*, 27(4), 363–390.

Ojeda, L., Kibangou, A., and de Wit, C. (2013). Adaptive kalman filtering for multi-step ahead traffic flow prediction. In *American Control Conference (ACC), 2013*, 4724–4729. doi:10.1109/ACC.2013.6580568.

Richards, P. (1956). Shockwaves on the highway. *Operations Research*, 4, 42–51.

Rosenberg, S., Vedlitz, A., Cowman, D.F., and Zahran, S. (2010). Climate change: a profile of us climate scientists perspectives. *Climatic Change*, 101(3-4), 311–329.

Saberi, M. and Mahmassani, H. (2012). Exploring properties of networkwide flow-density relations in a freeway network. *Transportation Research Record: Journal of the Transportation Research Board*, 2315, 153–163. doi:10.3141/2315-16. URL `http://dx.doi.org/10.3141/2315-16`.

Schrank, D.L., Eisele, B., and Lomax, T.J. (2012). *TTIs 2012 Urban Mobilty Report*. Texas Transportation Institute, Texas A & M University.

Vinberg, È.B. (2003). *A course in algebra*. 56. American Mathematical Soc.

Wu, X., Liu, H.X., and Geroliminis, N. (2011). An empirical analysis on the arterial fundamental diagram. *Transportation Research Part B: Methodological*, 45(1), 255 – 266. doi:http://dx.doi.org/10.1016/j.trb.2010.06.003.

Xie, X., Chiabaut, N., and Leclercq, L. (2013). Macroscopic fundamental diagram for urban streets and mixed traffic. *Transportation Research Record: Journal of the Transportation Research Board*, 2390, 1–10. doi:10.3141/2390-01. URL `http://dx.doi.org/10.3141/2390-01`.

Zarchan, P. and Musoff, H. (2005). *Progress In Astronautics and Aeronautics: Fundamentals of Kalman Filtering: A Practical Approach*, volume 208. Aiaa.

Zhang, L., Garoni, T.M., and de Gier, J. (2013). A comparative study of macroscopic fundamental diagrams of arterial road networks governed by adaptive traffic signal systems. *Transportation Research Part B: Methodological*, 49, 1–23.

Zheng, N., Waraich, R.A., Axhausen, K.W., and Geroliminis, N. (2012). A dynamic cordon pricing scheme combining the macroscopic fundamental diagram and an agent-based traffic model. *Transportation Research Part A: Policy and Practice*, 46(8), 1291 – 1303. doi: http://dx.doi.org/10.1016/j.tra.2012.05.006.